

The Cosmological Constant in the Quantum Multiverse

Grant Larsen, Yasunori Nomura, and Hannes L.L. Roberts

*Berkeley Center for Theoretical Physics, Department of Physics,
University of California, Berkeley, CA 94720, USA*

Theoretical Physics Group, Lawrence Berkeley National Laboratory, CA 94720, USA

Abstract

Recently, a new framework for describing the multiverse has been proposed which is based on the principles of quantum mechanics. The framework allows for well-defined predictions, both regarding global properties of the universe and outcomes of particular experiments, according to a single probability formula. This provides complete unification of the eternally inflating multiverse and many worlds in quantum mechanics. In this paper we elucidate how cosmological parameters can be calculated in this framework, and study the probability distribution for the value of the cosmological constant. We consider both positive and negative values, and find that the observed value is consistent with the calculated distribution at an order of magnitude level. In particular, in contrast to the case of earlier measure proposals, our framework prefers a positive cosmological constant over a negative one. These results depend only moderately on how we model galaxy formation and life evolution therein.

1 Introduction

An explanation of a small but nonzero cosmological constant is one of the major successes of the picture that our universe is one of the many different universes in which low energy physical laws take different forms [1]. Such a picture is also suggested theoretically by eternal inflation [2] and the string landscape [3]. This elegant picture, however, has been suffering from the predictivity crisis caused by an infinite number of events occurring in eternally inflating spacetime. To make physical predictions, we need to deal with these infinities and define physically sensible probabilities [4].

Recently, a well-defined framework to describe the eternally inflating multiverse has been proposed based on the principles of quantum mechanics [5]. In this framework, the multiverse is described as quantum branching processes viewed from a single “observer” (geodesic), and the probabilities are given by a simple Born-like rule applied to the quantum state describing the entire multiverse. Any physical questions—either regarding global properties of the universe or outcomes of particular experiments—can be answered by using this single probability formula, providing *complete unification* of the eternally inflating multiverse and many worlds in quantum mechanics. Moreover, the state describing the multiverse is defined on the “observer’s” past light cones bounded by (stretched) apparent horizons; namely, consistent description of the *entire* multiverse is obtained in these limited spacetime regions. This leads to a dramatic change of views on spacetime and gravity.

In this paper we present a calculation of the probability distribution of the cosmological constant in this new framework of the quantum multiverse.¹ We fix other physical parameters and ask what values of the cosmological constant Λ we are likely to observe. In Section 2 we begin by reviewing the proposal of Ref. [5], and we then explain how cosmological parameters can be calculated in Section 3. While the framework itself is well-defined, any practical calculation is necessarily approximate, since we need to model “experimenters” who actually make observations. In our context, we need to consider galaxy formation and life evolution therein, which we will do in Section 4. We present the result of our calculation in Section 5. We find that, in contrast to the case with some earlier measures [11], the measure of Ref. [5] does not lead to unwanted preference for a negative cosmological constant—in fact, a positive value is preferred. We find that a simple anthropic condition based on metallicity of stars is sufficient to make the calculated distribution consistent with the observed value at an order of magnitude level. We conclude in Section 6.

Appendix A lists formulae for galaxy formation used in our analysis. Appendix B discusses the anthropic condition coming from metallicity of stars.

¹For earlier studies of the cosmological constant in the context of geometric cutoff measures, see Refs. [6 – 10].

2 Probabilities in the Quantum Mechanical Multiverse

Here we review aspects of the framework of Ref. [5] which are relevant to our calculation. In this framework, the entire multiverse is described as a single quantum state as viewed from a single “observer” (geodesic). It allows us to make well-defined predictions in the multiverse (both cosmological and terrestrial), based on the principles of quantum mechanics.

Let us begin by considering a scattering process in usual (non-gravitational) quantum field theory. Suppose we collide an electron and a positron, with well-defined momenta and spins: $|e^+e^- \rangle$ at $t = -\infty$. According to the laws of quantum mechanics, the evolution of the state is deterministic. In a relativistic regime, however, this evolution does *not* preserve the particle number or species, so we find

$$\Psi(t = -\infty) = |e^+e^- \rangle \quad \rightarrow \quad \Psi(t = +\infty) = c_e |e^+e^- \rangle + c_\mu |\mu^+\mu^- \rangle + \dots, \quad (1)$$

when we expand the state in terms of the free theory states (which is appropriate for $t \rightarrow \pm\infty$ when interactions are weak). The Hilbert space of the theory is (isomorphic to) the Fock space

$$\mathcal{H} = \bigoplus_{n=0}^{\infty} \mathcal{H}_{\text{IP}}^{\otimes n}, \quad (2)$$

where \mathcal{H}_{IP} is the single-particle Hilbert space. Various “final states,” $|e^+e^- \rangle, |\mu^+\mu^- \rangle, \dots$, in Eq. (1) arise simply because the time evolution operator causes “hopping” between different components of the Fock space in Eq. (2).

The situation in the multiverse is quite analogous. Suppose the universe was in an eternally inflating (quasi-de Sitter) phase Σ at some early time $t = t_0$. In general, the evolution of this state is *not* along the axes determined by operators local in spacetime. Therefore, at late times, the state is a superposition of different “states”

$$\Psi(t = t_0) = |\Sigma \rangle \quad \rightarrow \quad \Psi(t) = \sum_i c_i(t) |(\text{cosmic}) \text{ configuration } i \rangle, \quad (3)$$

when expanded in terms of the states corresponding to definite semi-classical configurations. The Hilbert space of the theory is (isomorphic to)

$$\mathcal{H} = \bigoplus_{\mathcal{M}} \mathcal{H}_{\mathcal{M}}, \quad \mathcal{H}_{\mathcal{M}} = \mathcal{H}_{\mathcal{M},\text{bulk}} \otimes \mathcal{H}_{\mathcal{M},\text{horizon}}, \quad (4)$$

where $\mathcal{H}_{\mathcal{M}}$ is the Hilbert space for a fixed semi-classical spacetime \mathcal{M} , and consists of the bulk and horizon parts $\mathcal{H}_{\mathcal{M},\text{bulk}}$ and $\mathcal{H}_{\mathcal{M},\text{horizon}}$. (The quantum states are defined on the “observer’s” past light cones bounded by apparent horizons.) The final state of Eq. (3) becomes a superposition of different semi-classical configurations because the evolution operator for $\Psi(t)$ allows “hopping” between different $\mathcal{H}_{\mathcal{M}}$ in Eq. (4).

As discussed in detail in Ref. [5], any physical question can be phrased as: “Given what we know about our past light cone, A , what is the probability of that light cone to have properties B as well?” This probability is given by

$$P(B|A) = \frac{\int dt \langle \Psi(t) | \mathcal{O}_{A \cap B} | \Psi(t) \rangle}{\int dt \langle \Psi(t) | \mathcal{O}_A | \Psi(t) \rangle}, \quad (5)$$

assuming that the multiverse is in a pure state $|\Psi(t)\rangle$. (The mixed state case can be treated similarly.) Here, \mathcal{O}_A is the projection operator

$$\mathcal{O}_A = \sum_i |\alpha_{A,i}\rangle \langle \alpha_{A,i}|, \quad (6)$$

where $|\alpha_{A,i}\rangle$ represents a set of orthonormal states in the Hilbert space of Eq. (4), i.e. possible past light cones, that satisfy condition A (and similarly for $\mathcal{O}_{A \cap B}$). Despite the fact that the t integrals in Eq. (5) run from $t = t_0$ to ∞ , the resulting $P(B|A)$ is well-defined, since $|\Psi(t)\rangle$ is continually “diluted” into supersymmetric Minkowski states [5].

The formula in Eq. (5) (or its mixed state version) can be used to answer questions both regarding global properties of the universe and outcomes of particular experiments. This, therefore, provides complete unification of the two concepts: the eternally inflating multiverse and many worlds in quantum mechanics [5].² To predict/postdict physical parameters x , we need to choose A to select the situation for “premeasurement” *without* conditioning on x . We can then use various different values (ranges) of x for B , to obtain the probability distribution $P(x)$. In the next section, we discuss this procedure in more detail, in the context of calculating the probability distribution of the vacuum energy, $x = \rho_\Lambda \equiv \Lambda/8\pi G_N$.

3 Predicting/Postdicting Cosmological Parameters

In order to use Eq. (5) to predict/postdict physical parameters, we need to know the relevant properties of both the state $|\Psi(t)\rangle$ (or its bulk part $\rho_{\text{bulk}} \equiv \text{Tr}_{\text{horizon}} |\Psi(t)\rangle \langle \Psi(t)|$) and the operators \mathcal{O}_A and $\mathcal{O}_{A \cap B}$. Here we discuss them in turn.

In general, the state $|\Psi(t)\rangle$ depends on the dynamics of the multiverse, including the scalar potential in the landscape, as well as the initial condition, e.g. at $t = t_0$. Given limited current theoretical technology, this introduces uncertainties in predicting physical parameters. However, there are certain cases in which these uncertainties are under control. Consider $x = \rho_\Lambda$. We are

²The claim that the multiverse and many worlds are the same has also been made recently in Ref. [12], but the physical picture there is very different. Those authors argue that quantum mechanics has operational meaning only under the existence of causal horizons because making probabilistic predictions requires decoherence with degrees of freedom outside the horizons. Our picture does not require such an extra agent to define probabilities (or quantum mechanics). The evolution of our $\Psi(t)$ is deterministic and unitary.

interested only in a range a few orders of magnitude around $\rho_{\Lambda, \text{obs}} \simeq (0.0024 \text{ eV})^4$ [13], which is tiny compared with the theoretically expected range $-M_{\text{Pl}}^4 \lesssim \rho_{\Lambda} \lesssim M_{\text{Pl}}^4$. Therefore, unless the multiverse dynamics or initial condition has a special correlation with the value of the vacuum energy in the standard model (SM) vacua, we expect that the probabilities of having these vacua in $|\Psi(t)\rangle$ is statistically uniform in x within the range of interest. (This corresponds to the standard assumption of statistical uniformity of the prior distribution of ρ_{Λ} [1].) The distribution of $x = \rho_{\Lambda}$ is then determined purely by the dynamics *inside* the SM universes, i.e., the probability of developing experimenters who actually make observations of the vacuum energies.

Let us now turn to the operators \mathcal{O}_A and $\mathcal{O}_{A \cap B}$. In order to predict the value of the vacuum energy which a given experimenter will observe, we need to choose \mathcal{O}_A to select a particular “premeasurement” situation for that experimenter, i.e.

$$P(\rho_{\Lambda}) d\rho_{\Lambda} = P(B|A), \quad \begin{cases} A : & \text{a particular “premeasurement” situation} \\ B : & \rho_{\Lambda} < \text{vacuum energy} < \rho_{\Lambda} + d\rho_{\Lambda}, \end{cases} \quad (7)$$

where $P(B|A)$ is defined in Eq. (5). Here, we have assumed that the number of SM vacua is sufficiently large for ρ_{Λ} to be treated as continuous in the range of interest. In general, the specification of the premeasurement situation can be arbitrarily precise; for example, we can consider a particular person taking a particular posture in a particular room, with the tip of the light cone used to define $|\Psi(t)\rangle$ located at a particular point in space. In practice, however, we are interested in the vacuum energy “a generic observer” will measure. We therefore need to relax the condition we impose as A ; in other words, we need to “coarse grain” the premeasurement situation. In fact, some coarse graining is always necessary when we apply the formalism to postdiction (see discussions in Ref. [5]).

What condition A should we impose then? To address this issue, let us take the semi-classical picture of the framework, discussed in Section 2 of Ref. [5]. In this picture, the probability is given by

$$P(B|A) = \lim_{n \rightarrow \infty} \frac{\mathcal{N}_{A \cap B}}{\mathcal{N}_A}, \quad (8)$$

where \mathcal{N}_A is the number of past light cones that satisfy A and are encountered by one of the n geodesics emanating from randomly distributed points on the initial hypersurface at $t = t_0$. (This is equivalent to Eq. (5) in the regime where the semi-classical picture is valid.) Since we vary only ρ_{Λ} , all the SM universes look essentially identical at early times when the vacuum energy is negligible. The assumed lack of statistical correlation between ρ_{Λ} and the multiverse dynamics then implies that we can consider a fixed number of geodesics emanating from a fixed *physical* volume at an early time (e.g. at reheating) in these universes, and see what fraction of these geodesics find the “premeasurement” situation A in each of these universes.

Given that we are focusing on the SM universes in which only the values of ρ_{Λ} are different, it is reasonable to expect that all the experimenters look essentially identical for different ρ_{Λ} , at least

statistically—in particular, we assume that they have similar sizes, masses, and lifetimes. With this “coarse graining,” the condition A can be taken, e.g., as: the geodesic intersects with the body of an experimenter at some time during their life. In practice, this makes the probability proportional to the fraction of a fixed comoving volume at an early time that later intersects with the body of an observer. Note that the details of the condition A here do not matter for the final results—for example, we can replace the “body” by “head” or “nose” without changing the results because its effect drops out from the normalized probability. Thus, in this situation (and any situation in which condition A can be formulated entirely in terms of things directly encountered by the geodesic), the semi-classical approximation to the scheme of Ref. [5] can be calculated as the fat geodesic measure outlined in Ref. [14].³ We emphasize that the consistent quantum mechanical solution to the measure problem in Ref. [5] *forces* this choice on us.

We can now present the formula for $P(\rho_\Lambda)$ in a more manageable form. Since the probability for one of the geodesics to intersect an experimenter is proportional to the number of experimenters and the density of geodesics, we have

$$P(\rho_\Lambda) \propto \sum_{a \in \text{habitable galaxies}} N_{\text{obs},a} \rho_{\text{geod},a}, \quad (9)$$

where $N_{\text{obs},a}$ and $\rho_{\text{geod},a}$ are, respectively, the *total* number of observers/experimenters and the density of geodesics in a “habitable” galaxy a . Here, we have approximated that $\rho_{\text{geod},a}$ is constant throughout the galaxy a . Note that since we count *intersections* of experimenters with geodesics, rather than just the number of observers (as in much previous work, e.g. [6]), our results differ from such previous results by our factor of $\rho_{\text{geod},a}$. Our remaining task, then, is to come up with a scheme that can “model” $N_{\text{obs},a}$ and $\rho_{\text{geod},a}$ reasonably well so that the final result is not far from the truth.

4 Approximating Observers

In this section, we convert Eq. (9) into an analytic expression that allows us to compute $P(\rho_\Lambda)$ numerically. We focus on presenting the basic logic behind our arguments. Detailed forms of the functions appearing below, e.g. $F(M, t)$ and $H(t'; M, t)$, as well as useful fitting functions, are given in Appendix A.

Let us begin with $N_{\text{obs},a}$. We assume that, at a given time t , the number of observers arising in a given galaxy a is proportional to the total number of baryons in a

$$\frac{dN_{\text{obs},a}}{dt}(t) \propto N_{B,a}(t), \quad (10)$$

³To our knowledge, no detailed study of the probability distribution of the cosmological constant according to the fat geodesic measure has been published prior to this work.

as long as stars are luminous. This assumption is reasonable if the rate of forming observers is sufficiently small, which appears to be the case in our universe. To estimate the number of baryons existing in galaxies, we use the standard Press-Schechter formalism [15], which provides the fraction of matter collapsed into halos of mass larger than M by time t , $F(M, t)$. Since the amount of baryons collapsed is proportional to that of matter, we can use this function F to estimate the number of observers and find⁴

$$P(\rho_\Lambda) \stackrel{?}{\propto} - \int dt \int dM \frac{dF(M, t)}{dM} \rho_{\text{geod}}(M, t). \quad (11)$$

The expression of Eq. (11) does not take into account the fact that forming intelligent observers takes time, or that observers appear only when stars are luminous (which we postulate, motivated by the assumption that we are typical observers). To include these effects, we use the extended Press-Schechter formalism [16], which gives the probability $H(t'; M, t)$ that a halo of mass M at time t virialized before t' . The probability density $P(\rho_\Lambda)$ can then be written as

$$P(\rho_\Lambda) \stackrel{?}{\propto} - \int dt \int dM \frac{dF(M, t)}{dM} \{H(t - t_{\text{evol}}; M, t) - H(t - t_{\text{burn}}; M, t)\} \rho_{\text{geod}}(M, t), \quad (12)$$

where t_{evol} and t_{burn} are the time needed for intelligent observers to evolve and the characteristic lifetime of stars which limits the existence of life, respectively.

The density of geodesics $\rho_{\text{geod}}(M, t)$ is proportional to that of a dark matter halo of mass M at time t , which is given by its average virial density:

$$\rho_{\text{geod}}(M, t) \approx \left(\frac{dF(M, t_*)}{dM} \right)^{-1} \int_0^{t_*} dt' \rho_{\text{vir}}(t') \frac{d^2 F(M, t')}{dM dt'}, \quad (13)$$

where $t_* = \min\{t, t_{\text{stop}}(M)\}$ with $t_{\text{stop}}(M)$ the time after which the number of halos of mass M starts decreasing, i.e. when merging into larger structures dominates over formation of new halos: $d^2 F/dM dt|_{t=t_{\text{stop}}(M)} = 0$. (For the explicit expression of ρ_{vir} , see Appendix A.) In the interest of speeding up numerical calculation, we approximate this by the virial density at the time when the rate of matter collapsing into a halo of mass M , i.e. $-d^2 F/dM dt$, becomes maximum:

$$\rho_{\text{geod}}(M, t) \approx \rho_{\text{vir}}(\tau(M)), \quad (14)$$

where $\tau(M)$ is given by

$$\left. \frac{d^3 F(M, t)}{dM dt^2} \right|_{t=\tau(M)} = 0. \quad (15)$$

This approximation is indeed reasonable at the level of precision we are interested in: it works at the level of 20% for $t \gtrsim 1.7\tau(M)$ where the contribution to $P(\rho_\Lambda)$ almost entirely comes from.

⁴Note that the sign of dF/dM is negative because of the definition of F .

Finally, there will be several additional anthropic conditions for a halo to be able to host intelligent observers. For example, the mass of a halo may have to be larger than some critical value M_{\min} to efficiently form stars [17], and smaller than M_{\max} for the galaxy to be cooled efficiently [18, 19]. Considering these factors, we finally obtain from Eqs. (12) and (14)

$$P(\rho_\Lambda) = -\frac{1}{N} \int_{t_{\text{evol}}}^{t_f} dt \int_{M_{\min}}^{M_{\max}} dM \frac{dF(M, t)}{dM} \{H(t - t_{\text{evol}}; M, t) - H(t - t_{\text{burn}}; M, t)\} \rho_{\text{vir}}(\tau(M)) n(M, t), \quad (16)$$

where N is the normalization factor. Here,

$$t_f = \begin{cases} \infty & \text{for } \rho_\Lambda \geq 0 \\ t_{\text{crunch}} \equiv \sqrt{\frac{\pi}{6G_N|\rho_\Lambda|}} & \text{for } \rho_\Lambda < 0, \end{cases} \quad (17)$$

and we have put anthropic conditions besides $M_{\min, \max}$ in the form of a function n . Note that F , H , and ρ_{vir} (and possibly n) all depend on the value of the vacuum energy ρ_Λ ; see Appendix A.

In summary, $(dF/dM)(H|_{t-t_{\text{evol}}} - H|_{t-t_{\text{burn}}})n dM dt$ counts the (expected) number of observers in halos with mass between M and $M + dM$ at time between t and $t + dt$, and $\rho_{\text{vir}}(\tau)$ is proportional to the density of geodesics in such a halo and time, and so Eq. (16) gives the probability by counting their intersections (as in Eq. (9)), with n implementing some anthropic conditions. One well-motivated origin for n is metallicity of stars, which affects the rate of planet formation (see e.g. Refs. [20, 21]). Here we simply model this effect by multiplying some power m of integrated star formation up to time $t - t_{\text{evol}}$, which we assume to be proportional to the integrated galaxy formation rate for $M > M_{\min}$:

$$n(M, t) \propto (F(M_{\min}, \min\{t - t_{\text{evol}}, \tilde{t}_{\text{stop}}\}) - F(M, \min\{t - t_{\text{evol}}, \tilde{t}_{\text{stop}}\}))^m, \quad (18)$$

where \tilde{t}_{stop} is determined by $d\{F(M_{\min}, t') - F(M, t')\}/dt'|_{t'=\tilde{t}_{\text{stop}}} = 0$. (For the derivation of this expression, see Appendix B.) Motivated by the observation that the formation rate of certain (though not Earth-like) planets is proportional to the second power of host star metallicity [21], we consider the case $m = 2$, as well as $m = 1$.⁵

Another possible anthropic condition comes from the fact that if a halo is too dense, it may not host a habitable solar system because of the effects of close encounters [23]. Following Ref. [18], we assume this anthropic condition to take the form

$$n_\star \sigma_\dagger v_\dagger \lesssim \frac{1}{t_{\text{cr}}}, \quad (19)$$

⁵There is observational data for metallicity of galaxies in our universe [22], which our crude model here does not reproduce quantitatively. However, when we straightforwardly extrapolate the empirical data to other universes, the same regions of the integrand in Eq. (16) are suppressed/enhanced so that the effect on our calculation is qualitatively the same. It must be noted, though, that the strength of the effect may change; e.g. $P(\rho_\Lambda)$ for our model with $m = 1$ is qualitatively similar to the distribution obtained using the observation-motivated method with $m = 3$.

where n_* , σ_\dagger , v_\dagger , and t_{cr} are the density of stars, critical “kill” cross section, relative velocity of encounters, and some timescale relevant for the condition. Since $n_* \propto \rho_{\text{vir}}$, $v_\dagger \sim v_{\text{vir}} \propto M^{1/3} \rho_{\text{vir}}^{1/6}$, and σ_\dagger and t_{cr} are (expected to be) independent of M and ρ_{vir} , this is translated into

$$n(M, t) = \Theta\left(\tilde{\rho}_{\text{max}} - \rho_{\text{vir}}(\tau(M)) \left(\frac{M}{M_{\text{min}}}\right)^{2/7}\right), \quad (20)$$

where $\Theta(x)$ is the step function ($= 1$ for $x \geq 0$ and $= 0$ for $x < 0$), and we have normalized M by M_{min} .

The value of $\tilde{\rho}_{\text{max}}$ is highly uncertain. One way to estimate it is to follow Ref. [18] and take

$$n_* \sim (1 \text{ pc})^{-3} \left(\frac{\rho_{\text{vir}}}{\rho_{\text{vir,MW}}}\right), \quad \sigma_\dagger \sim \pi r_{\text{AU}}^2, \quad v_\dagger \sim v_{\text{vir}} \sim \sqrt{\frac{T_{\text{vir,MW}}}{m_p}} \left(\frac{M}{M_{\text{MW}}}\right)^{1/3} \left(\frac{\rho_{\text{vir}}}{\rho_{\text{vir,MW}}}\right)^{1/6}, \quad (21)$$

where m_p is the proton mass, $r_{\text{AU}} \simeq 1.5 \times 10^8$ km is the Sun-Earth distance, and $\rho_{\text{vir,MW}} \sim 2 \times 10^{-26}$ g/cm³, $T_{\text{vir,MW}} \sim 5 \times 10^5$ K, and $M_{\text{MW}} \sim 1 \times 10^{12} M_\odot$ are the virial density, virial temperature, and mass of the Milky Way galaxy, respectively. Using $t_{\text{cr}} \sim t_{\text{evol}} = 5$ Gyr, Eq. (19) leads to

$$\tilde{\rho}_{\text{max}} \sim 9 \times 10^3 \rho_{\text{vir,MW}} \left(\frac{M_{\text{MW}}}{M_{\text{min}}}\right)^{2/7} \sim 3 \times 10^{-22} \text{ g/cm}^3. \quad (22)$$

This corresponds to the constraint from direct encounters, i.e. the orbit of a planet being disrupted by the passage of a nearby star. There can also be a constraint from indirect encounters: a passing star perturbs an Oort cloud in the outer part of the solar system, triggering a lethal comet impact [18]. For a fixed M , this constraint can be about four orders of magnitude stronger than Eq. (22)

$$\tilde{\rho}_{\text{max}} \sim 3 \times 10^{-26} \text{ g/cm}^3; \quad (23)$$

namely, our Milky Way galaxy may lie at the edge of allowed parameter space.

In our analysis below, we consider either or both of the above conditions Eqs. (18) and (20). In the real world, there are (almost certainly) more conditions needed for intelligent life to develop. However, incorporating these conditions would likely improve the prediction/postdiction for ρ_Λ . In this sense, our analysis may be viewed as a “conservative” assessment for the success of the framework, although it is still subject to uncertainties coming from the modeling of observers.

5 Distribution of the Cosmological Constant

Our modeling of observers has several parameters which need to be determined phenomenologically: Eq. (16) contains M_{min} , M_{max} , t_{evol} , and t_{burn} , while Eq. (20) contains $\tilde{\rho}_{\text{max}}$. We take the “minimum” galaxy mass appearing in Eq. (16) to be

$$M_{\text{min}} = 2 \times 10^{11} M_\odot, \quad (24)$$

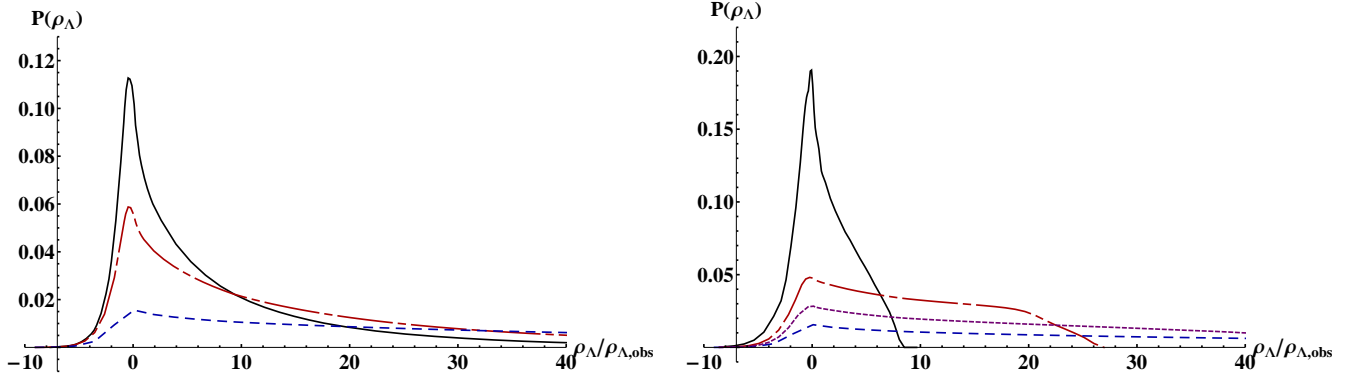


Figure 1: The normalized probability distribution of the vacuum energy $P(\rho_\Lambda)$ as a function of $\rho_\Lambda/\rho_{\Lambda,\text{obs}}$. The left panel shows $P(\rho_\Lambda)$ with the metallicity condition, Eq. (18), with $m = 0$ (i.e. no condition; dashed, blue), $m = 1$ (dot-dashed, red), and $m = 2$ (solid, black). The right panel shows $P(\rho_\Lambda)$ with the upper bound $\tilde{\rho}_{\text{max}}$, Eq. (20), with $\tilde{\rho}_{\text{max}} = \infty$ (i.e. no constraint; dashed, blue), 6×10^{-26} g/cm³ (dotted, purple), 4.5×10^{-26} g/cm³ (dot-dashed, red), and 3×10^{-26} g/cm³ (solid, black).

below which the efficiency of star formation drops abruptly [17]. For t_{evol} , and t_{burn} , we take them approximately to be the age of the Earth and lifetime of the Sun, respectively:

$$t_{\text{evol}} = 5 \text{ Gyr}, \quad t_{\text{burn}} = 10 \text{ Gyr}. \quad (25)$$

In our analysis below, we use Eqs. (24) and (25); we do not impose the constraint from galaxy cooling, i.e. we set $M_{\text{max}} = \infty$. While the values of these parameters are highly uncertain, our results are not very sensitive to these values. The dependence of our results on them will be discussed at the end of this section.

In Fig. 1, we present the normalized probability distribution for the vacuum energy $P(\rho_\Lambda)$ as a function of $\rho_\Lambda/\rho_{\Lambda,\text{obs}}$, under several assumptions about the function n :

- (i) “minimal” anthropic condition: $n(M, t) = 1$
- (ii) metallicity condition: Eq. (18) with $m = 1$ and 2
- (iii) maximum virial density condition: Eq. (20) with $\tilde{\rho}_{\text{max}} = \{3 \times 10^{-26}, 4.5 \times 10^{-26}, 6 \times 10^{-26}\}$ g/cm³, which are $\{1, 1.5, 2\}$ times the value in Eq. (23).

(The result with $\tilde{\rho}_{\text{max}}$ given by Eq. (22) is virtually identical to the case with the minimal anthropic condition.) The left panel presents the effects of metallicity, showing (i) and (ii), while the right panel those of $\tilde{\rho}_{\text{max}}$, with (i) and (iii).

Interestingly, in all cases, our predictions prefer a positive cosmological constant over a negative one, as opposed to the situation in earlier measure proposals where strong preferences to negative values have been found [11]. In Table 1, we provide the probabilities of having $\rho_\Lambda > 0$ (and < 0) in all six anthropic scenarios. The absence of an unwanted preference towards negative ρ_Λ is satisfactory,

	$P(\rho_\Lambda > 0)$	$P(\rho_\Lambda < 0)$
No condition	97%	3%
Metallicity, $m = 1$	87%	13%
Metallicity, $m = 2$	75%	25%
$\tilde{\rho}_{\max} = 6 \times 10^{-26} \text{ g/cm}^3$	92%	8%
$\tilde{\rho}_{\max} = 4.5 \times 10^{-26} \text{ g/cm}^3$	83%	17%
$\tilde{\rho}_{\max} = 3 \times 10^{-26} \text{ g/cm}^3$	63%	37%

Table 1: The probability of observing a positive and negative cosmological constant, $P(\rho_\Lambda > 0)$ and $P(\rho_\Lambda < 0)$, for six assumptions on the anthropic condition. In all cases, a positive value is preferred over a negative one, consistent with observation.

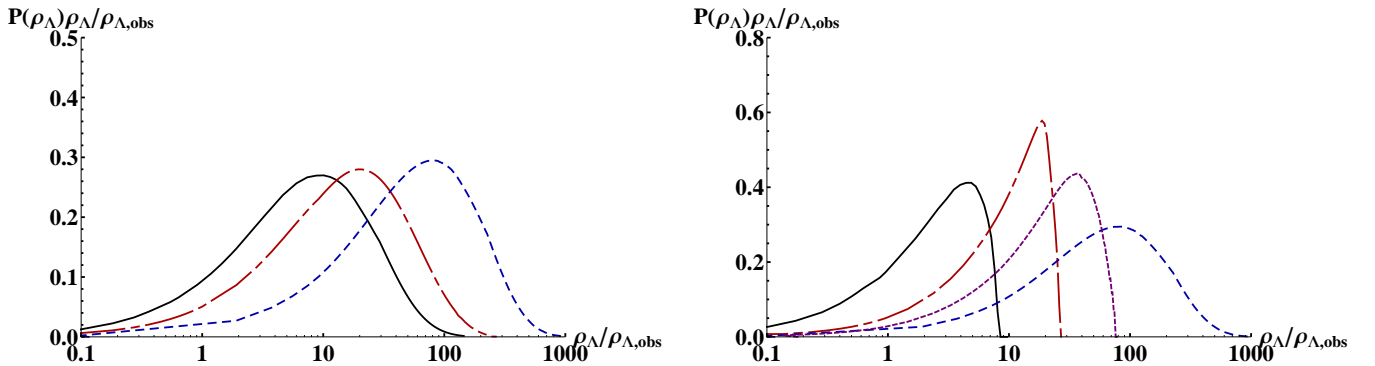


Figure 2: Same as Fig. 1, but the horizontal axis now in logarithmic scale. To show the probability density per tenfold, the vertical axis is chosen to be $\rho_\Lambda P(\rho_\Lambda)/\rho_{\Lambda,\text{obs}}$. The distributions are normalized in the region $\rho_\Lambda > 0$.

especially given that the measure of Ref. [5] was not devised to cure this problem. It comes from the fact that the present measure does not have a large volume effect associated with the global geometry of anti-de Sitter space, which was responsible for a strong preference for negative ρ_Λ in earlier, geometric cutoff measures [11]. In contrast with these measures, the quantum measure of Ref. [5] does *not* count the number of events; rather, it gives *quantum mechanical weights* for “situations,” i.e. quantum mechanical states as described from the viewpoint of a single observer (geodesic). The preference towards a positive value comes from the fact that for $\rho_\Lambda > 0$ some observers still form after vacuum energy domination, while for $\rho_\Lambda < 0$ it is not possible due to the big crunch.

Figure 1 shows that $P(\rho_\Lambda)$ is always peaked near $\rho_\Lambda = 0$, with the distribution becoming wider as the anthropic condition gets weaker. In Fig. 2, we plot the same distributions in logarithmic scale for $\rho_\Lambda/\rho_{\Lambda,\text{obs}}$, limiting ourselves to $\rho_\Lambda > 0$. To show the probability density per tenfold, the vertical axis is chosen as $\rho_\Lambda P(\rho_\Lambda)/\rho_{\Lambda,\text{obs}}$. From these figures, we find that our anthropic assumptions

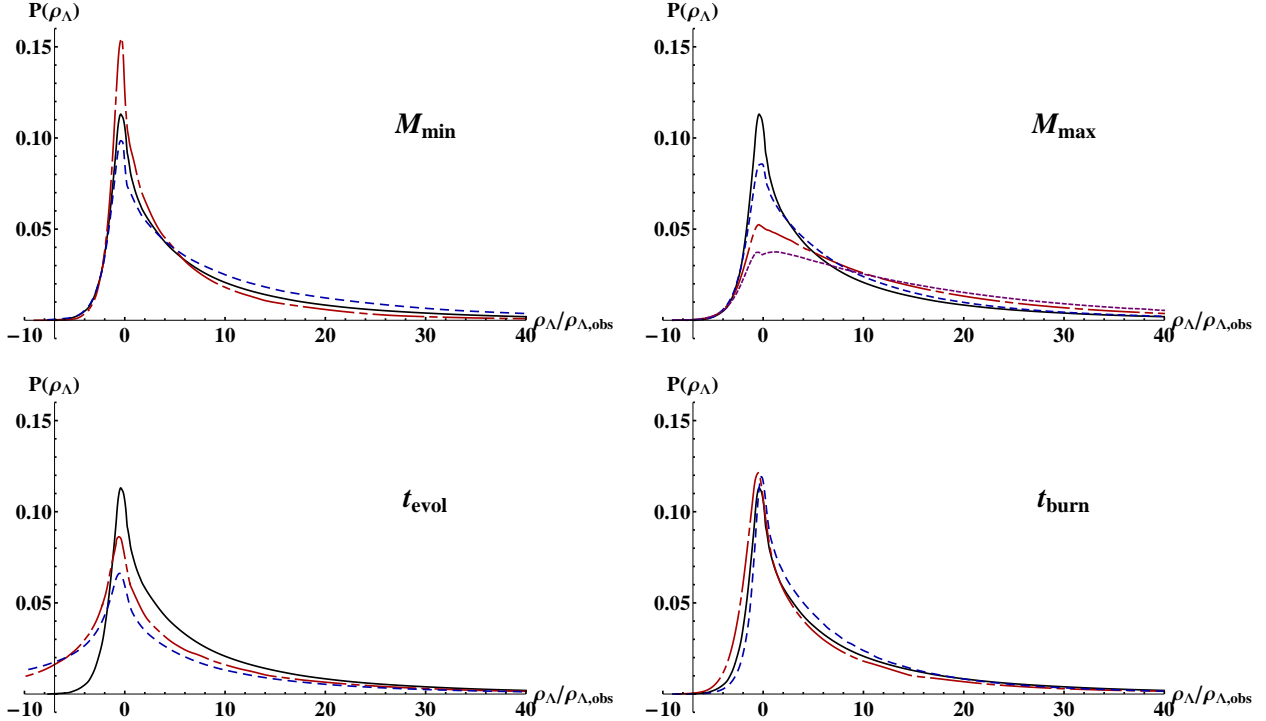


Figure 3: The normalized probability distribution $P(\rho_\Lambda)$ with the metallicity condition, Eq. (18), with $m = 2$. In the upper-left panel, M_{\min} is varied as $2 \times 10^{11} M_\odot$ (solid, black), $6 \times 10^{11} M_\odot$ (dot-dashed, red), and $0.67 \times 10^{11} M_\odot$ (dashed, blue); and in the upper-right, M_{\max} as ∞ (solid, black), $10^{14} M_\odot$ (dashed, blue), $10^{13} M_\odot$ (dot-dashed, red), and $2 \times 10^{12} M_\odot$ (dotted, purple). The lower left and right panels vary t_{evol} and t_{burn} as $\{(\text{solid, black}), (\text{dot-dashed, red}), (\text{dashed, blue})\} = \{5, 1, 0\}$ Gyr and $\{10, 7, 15\}$ Gyr, respectively.

lead to results that are consistent with the observed value within one or two orders of magnitude. In particular, metallicity alone is enough to bring the agreement to an order of magnitude level. This is because mergers, which lead to an increase in metallicity, are suppressed for larger values of ρ_Λ due to earlier vacuum energy domination. This result is comfortable, especially given that the constraint from encounters is effective only if $\tilde{\rho}_{\max}$ is close to the Milky Way value, as in Eq. (23). Given our crude treatment of observers, we consider these results quite successful.

Finally, we discuss the sensitivity of our results to variations of M_{\min} , M_{\max} , t_{evol} , and t_{burn} , which can be thought of as “systematic effects” of our analysis. In Fig. 3, we show the distributions of $P(\rho_\Lambda)$ with the $m = 2$ metallicity constraint, varying the values of M_{\min} , M_{\max} , t_{evol} , and t_{burn} , respectively. We find that, while the detailed shape of $P(\rho_\Lambda)$ does change, our main conclusions are robust: (i) There is no strong preference to a negative vacuum energy; in fact, a positive value is preferred. (ii) The predicted distribution of ρ_Λ is consistent with the observed value at an order of magnitude level with the metallicity constraint.

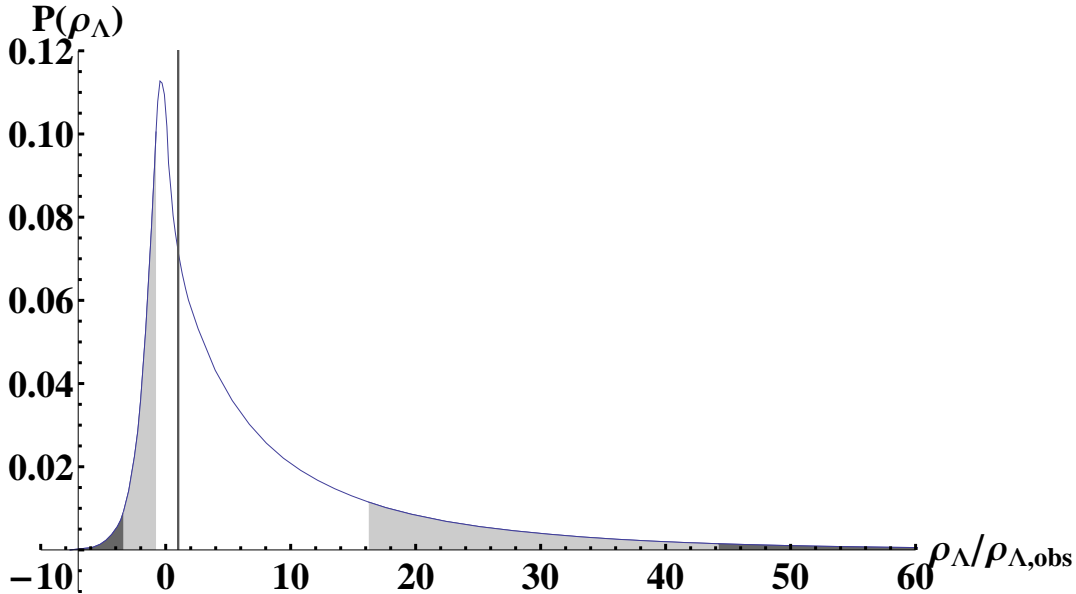


Figure 4: The normalized probability distribution $P(\rho_\Lambda)$ with a metallicity condition: Eq. (18) with $m = 2$. The light and dark shaded regions indicate those between 1 and 2σ , and outside 2σ , respectively. The observed value $\rho_\Lambda/\rho_{\Lambda,\text{obs}} = 1$ (denoted by a vertical line) is consistent with the distribution at the 1σ level.

6 Conclusions

In this paper, we have studied the probability distribution of the cosmological constant (or the vacuum energy ρ_Λ) in the multiverse, using the quantum measure proposed in Ref. [5]. We have found that this measure does not lead to a strong preference for negative ρ_Λ , as opposed to earlier measures proposed based on geometric cutoffs, because it does not experience a large volume effect associated with the global geometry of anti-de Sitter space. Moreover, we have found that a positive value of ρ_Λ is preferred, consistent with observation.

We have found that a simple, intuitive condition based on metallicity is enough to reproduce the observed value of ρ_Λ at an order of magnitude level. This is comfortable because effects from other possible anthropic conditions, such as the ones from encounters, are much more sensitive to the details of the conditions. In Fig. 4, we present the normalized distribution $P(\rho_\Lambda)$ with the $m = 2$ metallicity constraint, where the 1 and 2σ regions are indicated. We find that the observed value is consistent with the calculated distribution at the 1σ level.

It would be interesting to refine our analysis including more detailed anthropic effects, such as those of star formation. Another possible extension of the analysis is to vary other cosmological parameters, such as the primordial density contrast Q and spatial curvature Ω_k (at a specified time), in addition to ρ_Λ . We plan to study these issues in the future.

Acknowledgments

We thank Asimina Arvanitaki, Savas Dimopoulos, and David Pinner for useful discussions. This work was supported in part by the Director, Office of Science, Office of High Energy and Nuclear Physics, of the US Department of Energy under Contract DE-AC02-05CH11231, and in part by the National Science Foundation under grants PHY-0855653 and PHY05-51164.

A Press-Schechter Formalism and Fitting Functions

The Press-Schechter function F is

$$F(M, t) = \operatorname{erfc} \left(\frac{\delta_c(t)}{\sqrt{2} \sigma(M, t)} \right), \quad (26)$$

where $\delta_c(t)$ and $\sigma(M, t)$ are given by [18, 24]

$$\delta_c(t) \simeq \begin{cases} 1.629 + 0.057 e^{-2.3 G_N \rho_\Lambda t^2} & \text{for } \rho_\Lambda \geq 0 \\ 1.686 + 0.165 \left(\frac{t}{t_{\text{crunch}}} \right)^{2.5} + 0.149 \left(\frac{t}{t_{\text{crunch}}} \right)^{11} & \text{for } \rho_\Lambda < 0, \end{cases} \quad (27)$$

with t_{crunch} defined in Eq. (17), and

$$\sigma(M, t) \simeq Q s(M) G(t). \quad (28)$$

Here, Q is the primordial density contrast,

$$s(M) \simeq \left[(9.1 \mu^{-2/3})^{-0.27} + \{50.5 \log_{10}(834 + \mu^{-1/3}) - 92\}^{-0.27} \right]^{-1/0.27}, \quad (29)$$

where $\mu = M \xi^2 G_N^{3/2}$ with $\xi \equiv \rho_{\text{matter}}/n_\gamma \simeq 3.7$ eV, and

$$G(t) \simeq \begin{cases} 0.206 \frac{\xi^{4/3}}{\rho_\Lambda^{1/3}} \left[\tanh^{2/3} \left(\frac{3}{2} H_\Lambda t \right) \{1 - \tanh^{1.27} \left(\frac{3}{2} H_\Lambda t \right)\}^{0.82} \right. \\ \quad \left. + 1.437 \{1 - \cosh^{-4/3} \left(\frac{3}{2} H_\Lambda t \right)\} \right] & \text{for } \rho_\Lambda \geq 0 \\ 0.549 \xi^{4/3} G_N^{1/3} t^{2/3} \left[1 + 0.37 \left(\frac{t}{t_{\text{crunch}}} \right)^{2.18} \right]^{-1} \left[1 - \left(\frac{t}{t_{\text{crunch}}} \right)^2 \right]^{-1} & \text{for } \rho_\Lambda < 0, \end{cases} \quad (30)$$

where $H_\Lambda \equiv \sqrt{8\pi G_N |\rho_\Lambda|/3}$.

The function H in the extended Press-Schechter formalism is given by [16, 25]

$$H(t'; M, t) = - \int_{M/2}^M \frac{M}{M'} \frac{d\beta}{dM'} (M', t', M, t) dM', \quad (31)$$

where

$$\beta(M_1, t_1, M_2, t_2) = \operatorname{erfc} \left(\frac{1}{Q \sqrt{2(s(M_1)^2 - s(M_2)^2)}} \left(\frac{\delta_c(t_1)}{G(t_1)} - \frac{\delta_c(t_2)}{G(t_2)} \right) \right), \quad (32)$$

with $s(M)$ and $G(t)$ defined in Eqs. (29) and (30).

The virial density as a function of time can be fit, following Refs. [18, 25], as the density evolution of a closed universe, according to Birkhoff's theorem. The virial density is then given in terms of the density at turn-around rescaled by the ratio of the volumes, $\rho_{\text{vir}} = (R_{\text{vir}}/R_{\text{turn}})^3 \rho_{\text{turn}}$. Here, $R_{\text{vir}}/R_{\text{turn}} \rightarrow 2$ at early times ($t \ll 1/H_\Lambda$) as well as for $|\rho_\Lambda| \rightarrow 0$ at any fixed t . For positive ρ_Λ , $R_{\text{vir}}/R_{\text{turn}} = 2/(\sqrt{3} - 1) \simeq 2.73$ at late times [26], while for negative ρ_Λ , $R_{\text{vir}}/R_{\text{turn}} \rightarrow 2^{2/3}$ for $t \rightarrow t_{\text{crunch}}$. Our fit is given by

$$\rho_{\text{vir}}(t) \simeq \begin{cases} \left\{ \left(18\pi^2 \rho_{\text{matter}}(t) \frac{\sinh^2(\frac{3}{2}H_\Lambda t)}{(\frac{3}{2}H_\Lambda t)^2} \right)^{1.41} + (40.8 \rho_\Lambda)^{1.41} \right\}^{\frac{1}{1.41}} & \text{for } \rho_\Lambda \geq 0 \\ \left(18\pi^2 \rho_{\text{matter}}(t) \frac{\sin^2(\frac{3}{2}H_\Lambda t)}{(\frac{3}{2}H_\Lambda t)^2} \right) \frac{123.6}{123.6+7 \left(e^{4.14 \frac{t}{t_{\text{crunch}}}} - 1 \right)} & \text{for } \rho_\Lambda < 0, \end{cases} \quad (33)$$

where ρ_{matter} is the matter energy density. This fit is accurate to better than $\approx 5\%$ and 2% for $\rho_\Lambda \geq 0$ and < 0 , respectively.⁶

Finally, the time at which most of galaxies of mass M forms, i.e. the solution to Eq. (15), is well approximated by the following fitting function:

$$\tau(M)/\text{Gyr} \simeq \frac{Q_{\text{obs}}^{3/2}}{Q^{3/2}} \begin{cases} 1.880 + c_1(\alpha) \tilde{M} + c_3(\alpha) \tilde{M}^3 + c_5(\alpha) \tilde{M}^5 & \text{for } -10 \lesssim \frac{\rho_\Lambda}{\rho_{\Lambda, \text{obs}}} < 0 \\ c'_0(\alpha) + c'_1(\alpha) \tilde{M} + c'_3(\alpha) \tilde{M}^3 + c'_5(\alpha) \tilde{M}^5 & \text{for } 0 \leq \frac{\rho_\Lambda}{\rho_{\Lambda, \text{obs}}} < 10 \\ c''_0(\alpha) + c''_1(\alpha) \tilde{M} + c''_3(\alpha) \tilde{M}^3 + c''_5(\alpha) \tilde{M}^5 & \text{for } 10 \leq \frac{\rho_\Lambda}{\rho_{\Lambda, \text{obs}}} \lesssim 100, \end{cases} \quad (34)$$

where $\alpha = (\rho_\Lambda/\rho_{\Lambda, \text{obs}})(Q_{\text{obs}}/Q)^3$, $\tilde{M} \equiv \log_{10} \frac{M}{2 \times 10^{11} M_\odot}$, and

$$\begin{aligned} c_1(x) &= -0.311 + 1.276 e^{0.827x} + 1.412 \log_{10}\{1 + |x|^{0.7}\}, \\ c_3(x) &= 0.470 - 0.656 e^{0.78x} - 0.317 \log_{10}(0.2 + |x|), \\ c_5(x) &= -0.0142 + 0.0381 e^{0.7x} + 0.00822 \log_{10}(0.05 + |x|), \\ \\ c'_0(x) &= 1.880 - 0.00205 x, \\ c'_1(x) &= 0.408 + 0.569 e^{-1.01x} + 0.295 \log_{10}(1 + x), \\ c'_3(x) &= 0.277 - 0.251 e^{-x} - 0.125 \log_{10}(1 + x), \\ c'_5(x) &= -0.000889 + 0.0151 e^{-x} - 0.00220 \log_{10}(1 + x), \\ \\ c''_0(x) &= 1.880 - 0.00205 x, \\ c''_1(x) &= 0.767 - 0.00293 x - 230 x^{-4}, \\ c''_3(x) &= -0.530 + 0.000336 x + 0.847 x^{-0.1}, \\ c''_5(x) &= 0.106 - 0.0000118 x - 0.125 x^{-0.1} - 0.0131 \log_{10}(-5 + x). \end{aligned} \quad (35)$$

⁶For $\rho_\Lambda < 0$, the approximation leading to Eq. (33), i.e. $\rho_{\text{vir}} \gtrsim$ a few $(\rho_{\text{matter}} + \rho_\Lambda)$, breaks down for $t/t_{\text{crunch}} \gtrsim 0.8$, where we should rather use $\rho_{\text{vir}} = 0$ (since there is no stable structure forming). However, since ρ_{vir} in Eq. (33) is small there anyway, using it up to $t/t_{\text{crunch}} = 1$ does not lead to a significant error.

This fit is accurate to better than $\approx 5\%$ for $M \gtrsim 10^{11} M_\odot$ (but it becomes worse for smaller M , e.g., the accuracy is $\approx 12\%$ at $M \simeq 6 \times 10^{10} M_\odot$). For $100 < \rho_\Lambda/\rho_{\Lambda,\text{obs}} < 150$, we use the last expression of Eq. (34), good to the level of $\approx 10\%$; and for $\rho_\Lambda/\rho_{\Lambda,\text{obs}} > 150$, we use

$$\rho_{\text{vir}}(\tau(M)) / (10^{-26} \text{ g/cm}^3) \simeq (3.66 + 0.032 \alpha) - (1.36 + 0.0013 \alpha) \tilde{M}, \quad (36)$$

which is accurate to the level of $\approx 10\%$ up to $\rho_\Lambda/\rho_{\Lambda,\text{obs}} \approx 4500$.

B Anthropic Condition from Metallicity

In this appendix, we derive the function n arising from the metallicity constraint, Eq. (18). Suppose that in a merging tree of a galaxy j at time t , j is found to have progenitor galaxies $i = 1, 2, \dots$ with varying masses M_i at time $t' < t$. Note that this also includes accretion, i.e. matter that was not part of galaxies of appreciable size, since $F(M = 0, t) = 1$ in the Press-Schechter formalism, where accretion is treated as mergers of extremely tiny galaxies with a large galaxy.

Now, let us assume that the relative mass fraction in j that came from i and i' is given by $\frac{dF(M_i, t')}{dM_i} / \frac{dF(M_{i'}, t')}{dM_{i'}}$, i.e. the ratio of total amount of baryons at time t' in galaxies of type i and i' , respectively. This is true within the Press-Schechter formalism as long as $M_{i,i'} \ll M_j$, since then the overdensities within spherical top-hat regions containing masses $M_{i,i'}$ and M_j are independent of each other at early times. Once $M_{i,i'} \approx M_j$, the assumption is not justified, but in these regimes, there can only be a small amount of merging occurring from i, i' to j , implying little contribution to metallicity. The assumption, therefore, provides a good approximation.

Let x_i ($i = 1, 2, \dots$) be the fraction of baryons in the universe that formed stars in halos of mass M_i at time t' . In our simple model, the star formation rate is proportional to the rate of halo formation for masses $M > M_{\text{min}}$ and otherwise zero: $dx_i/dt' \propto \Theta(M_i - M_{\text{min}}) d^2 F(M_i, t')/dM_i dt'$. The increase in total metal content summed over galaxies of mass M_i is taken to be proportional to the star formation rate therein, dx_i/dt , so the increase in (linear) metallicity dZ_i is

$$dZ_i(t') \propto \left(\frac{dF(M_i, t')}{dM_i} \right)^{-1} \frac{dx_i}{dt'} dt' \propto \left(\frac{dF(M_i, t')}{dM_i} \right)^{-1} \frac{d^2 F(M_i, t')}{dM_i dt'} \Theta(M_i - M_{\text{min}}) dt', \quad (37)$$

i.e. the total increase in metal content divided by the total mass. The increase in metallicity of galaxy j due to stars at time t' , then, has to be weighted by the relative matter fraction of galaxies i , as described above:

$$dZ_j(t') = \frac{\sum_i \frac{dF(M_i, t')}{dM_i} dZ_i(t')}{\sum_i \frac{dF(M_i, t')}{dM_i}} \propto \frac{\sum_i \frac{d^2 F(M_i, t')}{dM_i dt'} \Theta(M_i - M_{\text{min}})}{\sum_i \frac{dF(M_i, t')}{dM_i}} dt', \quad (38)$$

where we must normalize to the total mass of galaxy j at each time t' .

In the continuum limit, the sum over i becomes an integral over masses. Therefore, the metallicity of galaxy j of mass M at time t is

$$Z(M, t) \propto \int_0^{\tilde{t}} dt' \frac{\int_0^M dM' \frac{d^2 F(M', t')}{dM' dt'} \Theta(M' - M_{\min})}{\int_0^M dM' \frac{dF(M', t')}{dM'}} = \int_0^{\tilde{t}} dt' \frac{\frac{d}{dt'} \{F(M_{\min}, t') - F(M, t')\}}{1 - F(M, t')}, \quad (39)$$

where $\tilde{t} = \min\{t, \tilde{t}_{\text{stop}}\}$. The constraint that one cannot accumulate negative metallicity determines the timescale \tilde{t}_{stop} as a solution to

$$\left. \frac{d}{dt'} \{F(M_{\min}, t') - F(M, t')\} \right|_{t'=\tilde{t}_{\text{stop}}} = 0, \quad (40)$$

at which time merging of galaxies of mass $M_{\min} < M' < M$ into those more massive than M begins to dominate over formation of new galaxies in this mass region. Since merging into larger structures is also occurring at earlier times, one expects that we slightly underestimate the metallicity. However, in practice, the formation of new galaxies in this mass range and mergers into structures beyond are well separated in time, so a simple cutoff at \tilde{t}_{stop} is sufficient.

Now, since $F(M, t') \leq F(M, \tilde{t}_{\text{stop}}) = \text{erfc}(1/\sqrt{2}) \simeq 0.317$, the denominator of Eq. (39) is always between 0.68 and 1; in fact, it is very close to 1 in most of the parameter regions. Therefore, we can safely ignore the denominator of Eq. (39) and obtain

$$Z(M, t) \propto (F(M_{\min}, \tilde{t}) - F(M, \tilde{t})). \quad (41)$$

In general, the probability of forming planets is expected to be proportional to some power m of the metallicity [20, 21]. This gives

$$n(M, t) = Z(M, t - t_{\text{evol}})^m, \quad (42)$$

which is Eq. (18) in the text.

References

- [1] S. Weinberg, Phys. Rev. Lett. **59**, 2607 (1987).
- [2] A. H. Guth and E. J. Weinberg, Nucl. Phys. B **212**, 321 (1983); A. Vilenkin, Phys. Rev. D **27**, 2848 (1983); A. D. Linde, Phys. Lett. B **175**, 395 (1986); Mod. Phys. Lett. A **1**, 81 (1986).
- [3] R. Bousso and J. Polchinski, JHEP **06**, 006 (2000) [arXiv:hep-th/0004134]; S. Kachru, R. Kallosh, A. Linde and S. P. Trivedi, Phys. Rev. D **68**, 046005 (2003) [arXiv:hep-th/0301240]; L. Susskind, arXiv:hep-th/0302219; M. R. Douglas, JHEP **05**, 046 (2003) [arXiv:hep-th/0303194].

- [4] For reviews, see e.g. A. H. Guth, Phys. Rept. **333**, 555 (2000) [arXiv:astro-ph/0002156]; A. Vilenkin, J. Phys. A **40**, 6777 (2007) [arXiv:hep-th/0609193]; S. Winitzki, Lect. Notes Phys. **738**, 157 (2008) [arXiv:gr-qc/0612164]; A. Linde, Lect. Notes Phys. **738**, 1 (2008) [arXiv:0705.0164 [hep-th]].
- [5] Y. Nomura, arXiv:1104.2324 [hep-th].
- [6] H. Martel, P. R. Shapiro and S. Weinberg, Astrophys. J. **492**, 29 (1998) [arXiv:astro-ph/9701099]; G. Efstathiou, Mon. Not. Roy. Astron. Soc. **274**, L73 (1995).
- [7] J. Garriga, M. Livio and A. Vilenkin, Phys. Rev. D **61**, 023503 (2000) [arXiv:astro-ph/9906210]; L. Pogosian and A. Vilenkin, JCAP **01**, 025 (2007) [arXiv:astro-ph/0611573].
- [8] R. Bousso, R. Harnik, G. D. Kribs and G. Perez, Phys. Rev. D **76**, 043513 (2007) [arXiv:hep-th/0702115]; J. M. Cline, A. R. Frey and G. Holder, Phys. Rev. D **77**, 063520 (2008) [arXiv:0709.4443 [hep-th]].
- [9] A. De Simone, A. H. Guth, M. P. Salem and A. Vilenkin, Phys. Rev. D **78**, 063520 (2008) [arXiv:0805.2173 [hep-th]].
- [10] R. Bousso, L. J. Hall and Y. Nomura, Phys. Rev. D **80**, 063510 (2009) [arXiv:0902.2263 [hep-th]].
- [11] M. P. Salem, Phys. Rev. D **80**, 023502 (2009) [arXiv:0902.4485 [hep-th]]; R. Bousso and S. Leichenauer, Phys. Rev. D **81**, 063524 (2010) [arXiv:0907.4917 [hep-th]]; R. Bousso, B. Freivogel, S. Leichenauer and V. Rosenhaus, arXiv:1012.2869 [hep-th].
- [12] R. Bousso and L. Susskind, arXiv:1105.3796 [hep-th].
- [13] E. Komatsu *et al.* [WMAP Collaboration], Astrophys. J. Suppl. **192**, 18 (2011) [arXiv:1001.4538 [astro-ph.CO]].
- [14] R. Bousso, B. Freivogel and I. S. Yang, Phys. Rev. D **79**, 063513 (2009) [arXiv:0808.3770 [hep-th]].
- [15] W. H. Press and P. Schechter, Astrophys. J. **187**, 425 (1974).
- [16] C. Lacey and S. Cole, Mon. Not. Roy. Astron. Soc. **262**, 627 (1993).
- [17] G. Kauffmann *et al.* [SDSS Collaboration], Mon. Not. Roy. Astron. Soc. **341**, 54 (2003) [arXiv:astro-ph/0205070].
- [18] M. Tegmark, A. Aguirre, M. J. Rees and F. Wilczek, Phys. Rev. D **73**, 023505 (2006) [arXiv:astro-ph/0511774].
- [19] A. Cattaneo, A. Dekel, J. Devriendt, B. Guiderdoni and J. Blaizot, Mon. Not. Roy. Astron. Soc. **370**, 1651 (2006) [arXiv:astro-ph/0601295].

- [20] C. H. Lineweaver, *Icarus* **151**, 307 (2001) [arXiv:astro-ph/0012399].
- [21] D. A. Fischer and J. Valenti, *Astrophys. J.* **622**, 1102 (2005); D. Grether and C. H. Lineweaver, *Astrophys. J.* **669**, 1220 (2007).
- [22] R. Maiolino *et al.*, *Astron. Astrophys.* **488**, 463 (2008) [arXiv:0806.2410 [astro-ph]]; P. S. Behroozi, C. Conroy and R. H. Wechsler, *Astrophys. J.* **717**, 379 (2010) [arXiv:1001.0015 [astro-ph.CO]].
- [23] M. Tegmark and M. J. Rees, *Astrophys. J.* **499**, 526 (1998) [arXiv:astro-ph/9709058].
- [24] J. A. Peacock, *Mon. Not. Roy. Astron. Soc.* **379**, 1067 (2007) [arXiv:0705.0898 [astro-ph]].
- [25] R. Bousso and S. Leichenauer, *Phys. Rev. D* **79**, 063506 (2009) [arXiv:0810.3044 [astro-ph]].
- [26] O. Lahav, P. B. Lilje, J. R. Primack and M. J. Rees, *Mon. Not. Roy. Astron. Soc.* **251**, 128 (1991).